A TOOL FOR GROUND DEFORMATION INVERSION USING 3D FINITE ELEMENT METHOD

Gilda Currenti
INGV- Sezione di Catania
Italy
currenti@ct.ingv.it

Alessandro Bonaccorso
INGV- Sezione di Catania
Italy
bonaccorso@ct.ingv.it

Ciro Del Negro
INGV- Sezione di Catania
Italy
delnegro@ct.ingv.it

Francesco Guglielmino
INGV- Sezione di Catania
Italy
gugliemino@ct.ingv.it

Danila Scandura
INGV- Sezione di Catania
Italy
scandura@ct.ingv.it

Charles A. Williams
GNS Science
New Zealand
C.Williams@gns.cri.nz

Abstract
Over the recent years, geodetic data, such as GPS displacements, DInSAR imagery, levelling and EDM measurements, has highlighted complex deformation pattern in proximity of active seismogenic structures. These patterns cannot be simply explained assuming uniform slip along the fault rupture but they are better modeled using heterogeneous slip distribution. To this aim, we developed an automated procedure for geodetic data inversion to estimate slip distribution along the fault ruptures. Finite Element Models are used to compute synthetic Greens functions for static displacements. FEM-generated synthetic Greens functions are then combined with inverse methods to estimate slip distributions that explain the observed ground deformation.

Key words
Geodetic inversion, numerical model, Mt Etna.

1 Introduction

Geodetic measurements have gained an important role in the monitoring of volcanic activity and in the quantitative evaluation of the geophysical processes preceding and accompanying volcanic unrest. During the last years, the higher spatial resolution of InSAR (Interferometric Synthetic Aperture Radar) data has been used to complement the coarse spatial resolution of GPS networks to obtain both accurate and fine spatial characterization of ground deformation. The large amount of available observations has definitely highlighted that slip along a fault rupture is usually not uniform and can be better described as a distribution of fault slips [Masterlark, 2003]. The overall displacement at an observation point is given by the superposition of contributions (Green's Functions) from each slip along the fault. The computation of the Green's functions is usually based on a homogeneous elastic half-space model, although medium heterogeneity and topography are likely to affect the magnitude and pattern of the deformation field [Currenti et al., 2008; Masterlark, 2003]. To account for real topography as well as heterogeneous material properties, we propose an automated procedure where the Finite Element Method (FEM) is implemented in inverse models to estimate slip distribution from geodetic observations. The procedure is applied to study the ground deformation observed on Mt Etna before the 2002-2003 eruption.

2 Numerical Procedure

The relationship between slip along a fault and ground displacements can be described by a linear relationship:

$$d_i = Gs \tag{1}$$

where G is the elastic response of the Earth (Green's functions), s is the fault slip and d_i are displacements observed at ground surface. Although uniform slip models can provide a fair fit to geodetic data, heterogeneous slip along the fault is expected. Subdividing the fault surface into M sub-faults (patches hereafter) leads to the displacement:

$$d_i = \sum_{j=1}^{n} G_{ij} s_i \tag{2}$$

where the G_{ij} coefficients are the contributions to the displacement at the i-th observation point due to a uni-

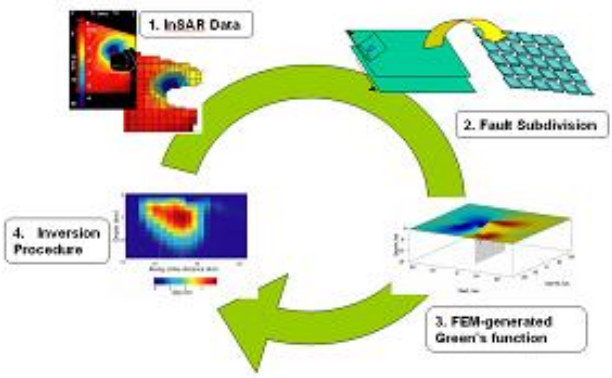

Figure 1. Schematic diagram of the main step in the automated procedure for InSAR data inversion.

tary dislocation along the j-th patch. Therefore, the inverse problem can be formulated as the solution of a system of N linear equations as:

$$\mathbf{d} = \mathbf{Gs} \tag{3}$$

where s is the M vector of unknown slip values along the patches, d is the N vector of observed ground displacements, and G is a matrix with elements G_{ij}. Summing up, the whole procedure can be split into three main sub-routines (Fig. 1) for: (i) meshing the computational domain and subdividing the fault in a finite number of patches; (ii) computing the Green's Functions for static displacements caused by unit slip over each patch using FEMs; (iii) solving an inversion problem to determine the slip distribution using a Quadratic Programming (QP) algorithm [Gill et al., 1981] with bound constraints on slip values. A description of the last two points is reported in the following paragraphs.

2.1 Finite Element Modeling

The Green's functions are computed using the finite-element method (FEM) to account for topographic effects as well as a complicated distribution of material properties. The numerical model is conducted using PyLith, a parallel finite element code [Williams, 2006]. The computational domain is a volume centered on Mt Etna and extending 100x100x50 km to avoid artifacts in the numerical solution because of the proximity of the external boundaries. For boundary conditions, the displacements on the outermost lateral boundaries and on the bottom are fixed to zero, while the boundary at the ground surface is free. The ground surface was generated from a digital elevation model of Mt Etna from the 90 m Shuttle Radar Topography Mission (SRTM) data and a bathymetry model from the GEBCO database (http://www.gebco.net/). Using LaGriT, a 3 D grid generation code from Los Alamos National Laboratory (http://lagrit.lanl.gov), the computational domain was meshed into 744886 isoparametric, and arbitrarily distorted tetrahedral elements connected by 129253 nodes. The mesh resolution is about 100 m around the seismogenic structures, about 500 m in the 20 x 20 km area around the summit craters and decreases to 2 km in the far field.The elastic parameters were inferred from seismic wave velocities using results of tomography investigations [Patane et al., 2006]. The subsurface elastic heterogeneities of the medium were included in the numerical model by assigning to each element in the meshed domain the value of the elastic Young's elastic modulus interpolated at the element location. Using a medium density of 2500 kg/m^3, the Young modulus varies in the range from 11.5 GPa at shallower depth to 133 GPa at greater depth. Slip along the fault surface is implemented by means of cohesive elements [Williams, 2006]. The computation of the G matrix for the M fault patches requires M x 3 (for strike-slip, dip-slip and tensile kinematics) model runs.

2.2 Geodetic Inversion

The inverse problem consists in minimizing the difference between the observed ground deformation and that calculated using the forward model (eq. 4). Linear least-squares methods for this problem require to incorporate regularization techniques in order to stabilize the problem and to reduce the set of likely solution. The inverse solution can yield irregular slip values on adjacent patches. Although this slip model may well fit the data, it is unrealistic. The reduction of the class of possible solutions to some set on which the solution is stable lies in the fundamental concept of introducing a regularizing operator. The inverse problem can be re-formulated as an optimization problem aimed at finding the unknown slip values s that minimize a data misfit ϕ_d and a smoothing functional ϕ_r defined as:

$$\phi = \phi_d + \lambda\phi_r = \frac{1}{2}[(\mathbf{d} - \mathbf{d}_{obs})^T(\mathbf{d} - \mathbf{d}_{obs})] + \lambda\phi_r \tag{4}$$

where λ is a regularization parameter, namely a trade-off between minimizing a measure of the data misfit ϕ_d and the smoothing functional ϕ_r. To avoid large variations between adjacent patches, a smoothing functional is used in a way to minimize the second-order spatial derivative (Laplacian) of the slip distribution:

$$\phi = \frac{1}{2}[(\mathbf{Gs} - \mathbf{d}_{obs})^T(\mathbf{Gs} - \mathbf{d}_{obs})] + \lambda\mathbf{s}^T\mathbf{L}^T\mathbf{Ls} \tag{5}$$

The Laplacian Operator L is computed using a finite-difference method [Masterlark, 2003]. Since λ controls the sensitivity of the regularized solution, it should be chosen so that a good balance is assigned to the smoothing functional, thereby warranting that the observations are well reproduced by the model. Among

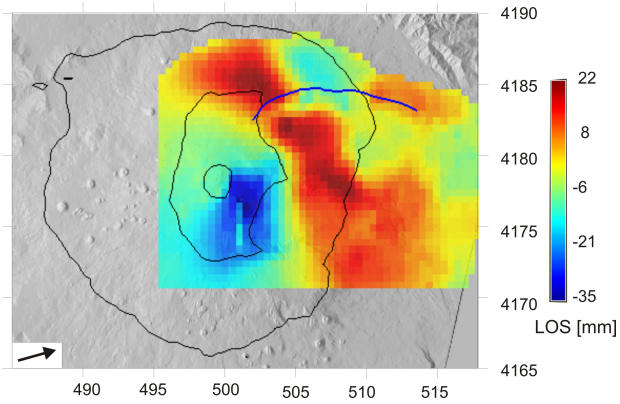

Figure 2. Unwrapped interferogram in the line of sight (LOS) to the satellite.

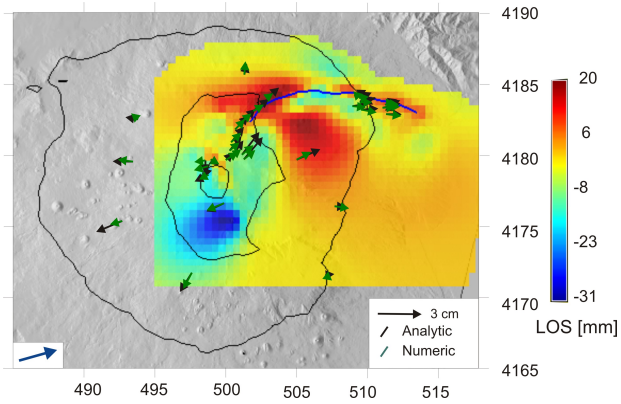

Figure 3. Computed displacement in the line of sight (LOS) to the satellite. Analytical and numerical solutions of the horizontal displacements are shown with arrows.

the several techniques that have been developed to properly estimate in inverse problem we used the L-curve criterion [Napoli et al., 2007]. To ensure reasonable solutions from the minimization of the functional in eq. 5, it is advisable to prescribe realistic bounds on slip values. The minimization of the quadratic functional subjected to bound constraints can be solved by using a Quadratic Programming (QP) algorithm based on an active set strategy [Gill et al., 1981]:

$$min\phi = min[\frac{1}{2}\mathbf{s}^T\mathbf{Q}\mathbf{s} - \mathbf{f}^T\mathbf{s}], \mathbf{L} <= \mathbf{s} <= \mathbf{U} \quad (6)$$

where $\mathbf{Q} = \mathbf{G}^T\mathbf{G} + \lambda\mathbf{L}^T\mathbf{L}$ and $\mathbf{f} = \mathbf{G}^T\mathbf{d}$, and $\mathbf{L}$ and $\mathbf{U}$ are the vectors of lower and upper bounds on slip values. The quadratic formulation of the problem is solved iteratively by generating a sequence of feasible solutions that converge toward the optimal solution. The iteration is stopped when no relative improvements in the functional are achieved.

3 Model Results and Discussion

The presented procedure is applied to study the ground deformation observed on Mt Etna before the 2002-2003 eruption. On 22 September 2002, an M3.7 earthquake, whose epicenter was located a few kilometers south of the westernmost part of the Pernicana fault, struck the northeastern part of Mt Etna volcano. This event produced coseismic surface fractures and damage to manmade features. The comparison between the results of the GPS survey carried out in September and in July 2002 showed a ground deformation pattern that affected the whole northeastern flank of the volcano [Bonforte et al., 2007]. The unwrapped interferogram (Fig. 2) was obtained from two ascending ERS2 passes taken on 31 July and 9 October 2002.

Both InSAR and GPS data showed a ground deformation pattern which revealed a general eastward motion of the northeastern sector of the volcano [Bonforte et al., 2007]. A GPS data inversion based on homogeneous half-space models predicted dislocation sources that were not able to reliably predict the complex deformation pattern detected by InSAR data. This discrepancy reflects the oversimplifications in the GPS fault model and the need to use better deformation models. We use InSAR observations and FEM-based models to estimate the slip distribution along the surface ruptures.

The fault surfaces, which represent the main seismogenic faults in the northeastern sector of Mt Etna, were divided into 248 patches requiring 744 FEM simulations to compute the Green's functions for the three fault slip components (dip-slip, strike-slip and tensile-opening). Then, we inverted the InSAR observations for the fault slip distribution using the QP algorithm [Gill et al., 1981] and obtained models that minimized the data misfit while preserving smoothness of the fault slip distribution (Fig. 2). The heterogeneous distribution of the slip along the structure is able to match the DInSAR image. The LOS residuals have an almost null mean (0.1 mm) and a Root Mean Square Error (RMSE) of about 7 mm. The retrieved slip distributions on the faults are shown in Fig. 3. The results show complex kinematics on the north-eastern flank of the volcano involving the main seismogenic structures.

The numerical model highlights a heterogeneous slip distribution along the fault surfaces with a predominant strike-slip mechanism associated with a dip-slip movement in the western part. A heterogeneous distribution of the slip along the structures is able to better justify the InSAR ground deformation and also matches the GPS observations. The proposed procedure, based on the use of a FEM model and the integrated inversion of InSAR and GPS data, provides a powerful tool to estimate fault movements and predict ground deformation in a complex geomechanical system.

References

Bonforte, A., Gambino, S., Guglielmino, F., Obrizzo, F., Palano, M. and Puglisi, G. (2007) Ground defor-

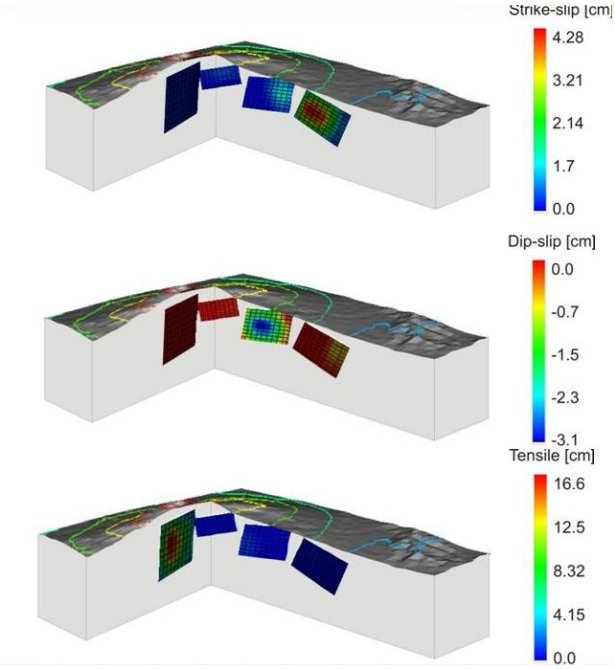

Figure 4. Slip distributions along the seismogenic faults on the north-eastern flank of Mt Etna.

mation modeling of flank dynamics prior to the 2002 eruption of Mt. Etna. *Bull. Volcanol.* , (69), pp. , 757–768.

Currenti, G., Del Negro, C., Ganci, G. and Scandura, D. (2008) 3D numerical deformation model of the intrusive event forerunning the 2001 Etna eruption. *Phys. Earth Plan. Int.* , (168), pp. , 88–96.

Gill, P. E., Murray, W. and Wright M. H. (1981). *IPractical Optimization*. Academic Press. London.

Napoli, R., Currenti, G. and Del Negro, C. (2007) Internal structure of Ustica volcanic complex (Italy) based on a 3D inversion of magnetic data. *Bull. Volcanol.* , (168), pp. , 869-879.

Masterlark T. (2003) "Finite element model predictions of static deformation from dislocation sources in a subduction zone: Sensitivities to homogeneous, isotropic, Poisson-solid, and half-space assumptions. *J. Geophys. Res.* , (108), pp. , 2540–2556.

Patane, D., Barberi, G.,Cocina, O., De Gori, P. and Chiarabba C. (2006) Time-resolved seismic tomography detects magma intrusions at Mount Etna. *Science* , (313), pp. , 821–823.

Williams, C. A. (2006) Development of a package for modeling stress in the lithosphere. *Eos Trans. AGU* , (87), pp. , 36.